Uotinen, Lauri; Torkan, Masoud; Janiszewski, Mateusz; Baghbanan, Alireza; Nieminen, Ville; Rinne, Mikael

Characterization of hydro-mechanical properties of rock fractures using steady state flow tests

Published in:
ISRM International Symposium - EUROCK 2020

Published: 13/11/2020

Document Version
Publisher's PDF, also known as Version of record

Norwegian Group for Rock Mechanics
ISBN: 978-82-8208-072-9
C.C. Li, H. Ødegaard, A.H. Høien, J. Macias (Eds.)

ISRM International Symposium
Eurock 2020 – Hard Rock Engineering
Trondheim, Norway, 14-19 June

Characterization of hydro-mechanical properties of rock fractures using steady state flow tests

L. Uotinen[1], M. Torkan[1], M. Janiszewski[1], A. Baghbanan[1,2], V. Nieminen[1] & M. Rinne[1]
[1)] *Aalto University, Espoo, Finland*
lauri.uotinen@aalto.fi
[2)] *Isfahan University of Technology, Isfahan, Iran*

Abstract

Characterization of Hydro-Mechanical (H-M) properties of rock fractures is the initial and important step in modeling of fully H-M coupled processes in fractured rock masses. Fluid flow in the fractured rock mass is an important aspect when evaluating the safety of geological disposal of high-level nuclear waste. Many attempts have been taken to measure and model fluid flow in rock fractures in different stress field conditions. However, still study about the scale effect of fracture properties and confinement stress on the conductivity of rough rock fractures remains a challenging topic of research. As a part of an ongoing research project about fluid flow modeling in fractured rock mass (RAKKA), and as an initial step one rock slab pair with sizes of 250 mm x 250 mm of Kuru grey granite halves was prepared. It has a horizontal mechanically induced tensile fracture. The surface roughness of the fracture was mapped using a conventional profilometer and structure-from-motion photogrammetry before each fluid flow test. The fractures were subjected to different normal stress and then fluid flow within the fractures was conducted linearly from edge to opposite edge with perpendicular edges sealed, and conductivity of the fractures under steady-state condition was measured. Then the test is repeated with all three sides open. The results show anisotropic behaviour in permeability. The diagonal components of the permeability matrix are significantly stress-dependent. Together the new fracture digitization method and the new three-way fluid flow test allow the contactless characterization of hydro-mechanical properties of rock fractures and the validation of the results.

Keywords

Rock fracture, fluid flow, stress-flow coupling, scale effect, stress effect

ISRM

NBG

1 Introduction

Deep underground nuclear waste repository is regarded as the most acceptable solution for the management of spent nuclear fuel and it is the present plan in Finland for high-level nuclear waste management. The repository comprises several engineered barriers to prevent the release of radionuclides to the surrounding environment. The bedrock is the final barrier for escaping radionuclides and fluid flow in fractures of the bedrock is a hydromechanically coupled rock engineering problem where fluid pressure can open fractures and rock stress can close fractures.

Fluid flow in a single fracture in fractured rock masses is studied extensively by several authors (e.g. Brown et al. 1998, Isakov et al. 2001, Zimmerman & Main 2004, Ogilvie et al. 2006, Yasuhara et al. 2006, Ferer et al. 2011). Also, a number of experimental studies have been carried out where the effects of three-dimensional stress field to a fluid flow through rock fracture are studied (e.g. Barton & Choubey 1977, Bandis et al. 1981, Yeo et al. 1998, Lee et al. 2002, Min et al. 2004, Jiang et al. 2004, Saito et al. 2005, Li et al. 2008, Nemoto et al. 2009, Rong et al. 2016, Wang et al. 2019). Flow properties of small-scale rock fractures are well studied, which creates the need to move towards larger scale to further validate the results acquired from small-scale laboratory studies.

RAKKA project is a continuation of the KARMO project (2014 – 2018), which created a photogrammetric method to measure and record the rock fracture surfaces with high precision. Firstly, the motivation for the research is to create data for numerical analysis for defining the flow properties of fracture networks. The properties of single fractures are input data in the numerical modelling of larger fracture networks. Secondly, the research aims to create knowledge about the phenomena in bedrock since the stability of the bedrock as well as the flow properties of the bedrock are important aspects when judging the safety of the repository. This knowledge then can be used in evaluating different methods and implementation of nuclear waste management. An important part of this research is to construct an experimental set up for three-way fluid flow tests. The obtained experimental data can be used to validate the numerical modelling results of the digitized geometry.

The basis of bedrock permeability is in the microstructure of the rock. The rock mass is a porous material that comprises mineral grains that are forming a lattice. Fractures are also part of a rock mass and fractures can be found at all scales down to the size of the mineral structure. It can be said that the bedrock comprises rock mass combined with fractures and they both contribute to the flow. Flow in the fractures is usually faster than in the rock and the differences in permeability of rock and fractures can be many orders of magnitude. It is crucial to understand thoroughly the behaviour of a single fracture before the behaviour of fractured rock masses can be understood (Jaeger et al. 2007).

The flow path of groundwater varies when the stress field in bedrock undergoes changes, and on the other hand, groundwater alters the effective stress state in rock fractures. Fluid affects the stress state in the rock and thus can create new flow paths and the stress state affects the opening and closing of the flow paths as well the fracture aperture. The situation can be regarded as a connected hydromechanical problem. In terms of nuclear waste management, hydromechanical modelling is part of thermos-hydro-mechanic-chemical modelling. The connected hydromechanical problem has a two-way connection so it can be viewed separately from temperature and chemical processes when not operating in the immediate vicinity of the repository tunnels. The hydromechanical processes of a single rock joint are dependent on the rock joint properties and the connected rock joint properties, geometry, orientation and the effective stress of the fracture walls (Zimmermann & Main 2004).

Fractured rock masses comprise intact rock blocks and fractures, which work as main pathways for fluid flow and fracture aperture can vary either due to closures induced by normal stress or openings or due to shear stress-induced dilations (Min et al. 2004). According to Rutqvist & Stephansson (2003), the hydromechanical coupling can be either indirect, where the applied stresses produce changes in the hydraulic properties of the rock or direct, where the applied stresses produce changes in fluid pressure. The indirect hydromechanical coupling can be seen as particularly important in fractured rock masses because stress-induced alterations in permeability can be up to several orders of magnitude and irretrievable (Min et al. 2004). It is a common conception that horizontal stress is the maximum principal stress at least in shallow bedrock (Şen & Sadagah 2002). Hydraulic properties depend on the mechanical loading conditions, which means that the hydraulic characteristics are almost completely coupled to the mechanical behaviour of fractures (Noorishad & Tsang 1996, Lee & Cho 2002).

2 Methodology

In order to investigate joint hydraulic properties, this study attempts to consider real situations existing in the field, namely different rock joint roughness, non-identical stress conditions, a wide verity of water pressures and flow directions. The experimental workflow is as follows: roughness measurements using profilometer (2.1), roughness measurements using photogrammetry (2.2), water flow tests (2.3), back-calculation of hydraulic aperture (2.4), comparison of the predictions based on roughness and the measurements from the water flow tests (2.5).

2.1 Roughness measurements using a profilometer

JRC (joint roughness coefficient) plays a key role in appraising the roughness of joints (Barton and Choubey 1977). Joint surface roughness can be defined for example according to undulation and irregularities of joint surface (ISRM 1978). Rock slab pairs with sizes of 250 mm × 250 mm of Kuru grey granite were prepared as shown in Fig. 1. According to ISRM 1978, the roughness of the joint surfaces of the RAKKA sample was measured using a profilometer. For the rock block, there were 6 measurement lines for each joint surface with 3 lines in the X direction and 3 lines in the direction Y, respectively, as presented in Fig. 2. Top and bottom sides were measured separately and there are in total 12 measurement lines for each slab pair.

2.2 Roughness measurements using photogrammetry

The rock joint surfaces were photographed with a photogrammetric prediction of the joint roughness according to the 3D model of the joint surface. The idea is to capture the whole fracture surface of the sample from every side with two dip angles of 30° and 60° and to reconstruct the fracture surface using the Structure-from-Motion photogrammetric method. The camera was mounted on a tripod in a fixed position and the sample was placed on a rotating platform (Fig. 3a). Two L-shaped scale bars with 20-bit circular markers spaced at 250 mm were positioned at sides of the rock sample for scaling. The platform was rotated in increments of 9 degrees with a picture taken after each rotation. The photographs were taken using Canon 5DS R DSLR camera and Canon 35 mm f/1.4L II USM objective. After a full 360° rotation, the camera height and vertical angle were adjusted, and the process repeated to produce two 369° loops with 41 pictures each (Fig. 3b).

Fig. 1. Kuru gray granite slab pair 250 mm x 250 mm x 110 mm.

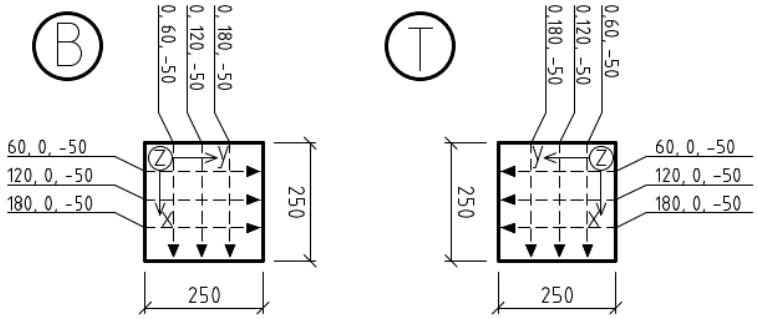

Fig. 2. Roughness measurement lines for the fracture surfaces of the small rock blocks. The view direction is toward the fracture surface and the B and T markings represent bottom and top slab respectively.

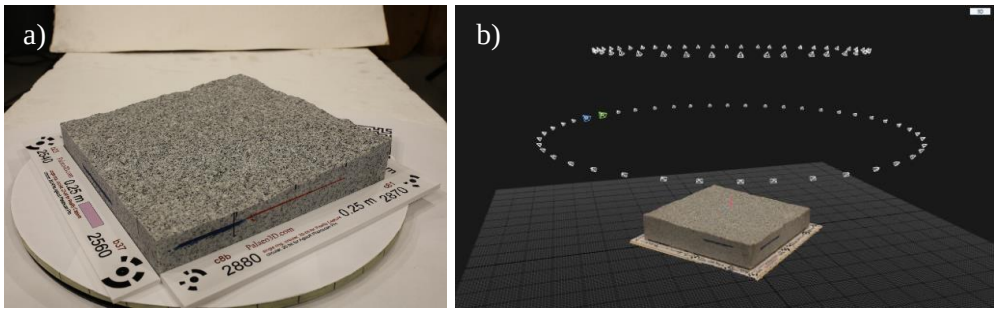

Fig. 3. Photogrammetry using a rotating platform and 250 mm scale bars (a) and camera positions (b).

The 82 photograph set was imported into RealityCapture 1.0.3.9303 photogrammetry software and the images were aligned using the default settings. Next, the dense 3D point cloud of the sample was

reconstructed using the Normal detail mode. The 3D model was scaled using the known distance between the circular markers on the scale bars, and the point cloud was colorized. Next, the point cloud was saved as a .xyz file and imported into CloudCompare v2.10.1 software to extract the roughness profiles. For this purpose, the Extract sections function was used that enables to extract cloud sections along polylines. Three parallel profile pairs in both X and Y directions were extracted from 3D point clouds of the bottom and the top fracture surfaces.

2.3 Water flow tests

To set up the test, a frame was built (Figs. 4 and 5). The frame was designed to investigate flow paths to multiple directions as in the actual conditions, fluid can enter and leave from different edges. Water pressures 1 bar, 3 bar and 5 bar were elected to conduct this experiment using a Kytola pressure meter. The four faces of the frame were sealed by the rubber to provide the hydraulic connection and controlled by valves to be selected water flow directions. Silicon glue and tape were used to seal the corners of the sample.

2.4 Back-calculation of hydraulic aperture

The conductivity was measured in along direction X with direction Y sealed (Fig. 5a). Then a three-way flow test was conducted; water was allowed to seep through the sides of direction X in addition to the two sides in direction Y (Fig. 5b). The water dripped from three sides was collected to measure the total conductivity. The identical approach was employed in direction Y (Figs. 5cd).

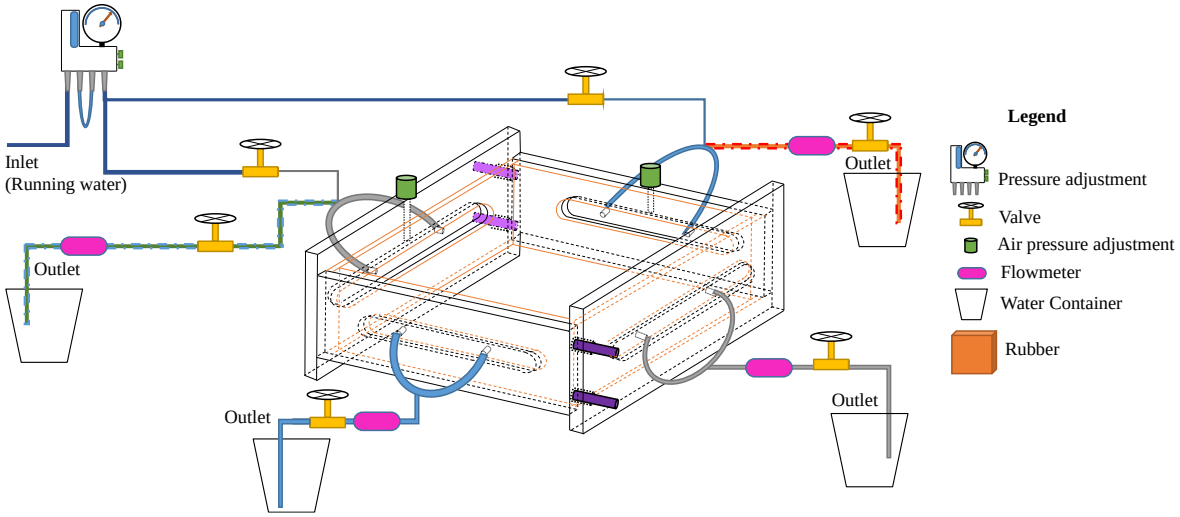

Fig. 4. Diagram indicating the functioning principle of the three-way flow test.

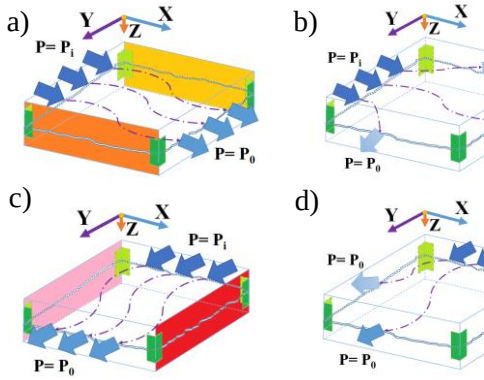

Fig. 5. Fluid flows without normal stress in the joint in direction X and sealing direction Y (a), in direction X and collecting water from other sides (b), in direction Y and sealing direction X (c), in direction Y and collecting water from other sides (d).

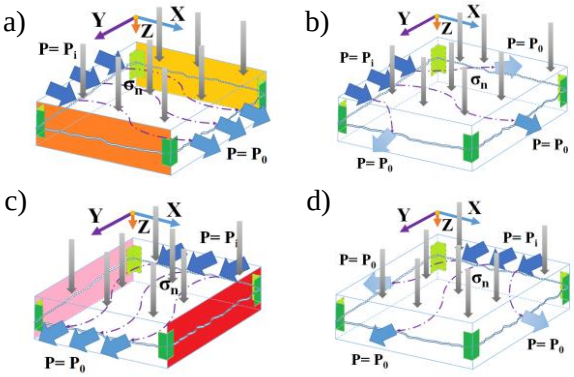

Fig. 6. Normal stress applied and fluid flows in the joint in direction X and sealing direction Y (a), in direction X and collecting water from other sides (b), in direction Y and sealing direction X (c), in direction y and collecting water from other sides (d).

According to Lee & Cho (2002), the relation between mechanical aperture and hydraulic aperture is fairly linear under normal loading but as the normal stress increases and the mechanical aperture becomes smaller, the corresponding hydraulic aperture diverges from the linear development which is concluded to be caused by more tortuous flow paths at high-stress levels. For the study of the stress magnitude effect, the sample was loaded with a normal force of 12.5 kN resulting in normal stress of

0.2 MPa, with the same situations as analysing conductivity for each step (Figs. 6a-6d). The load was applied using a load cell with a load evening 200 mm x 200 mm x 20 mm steel plate. The uplift was restricted by metal rods connected to a stiff frame. For each rock fracture specimen, if the flow rate in outlet of fracture is stable, the hydraulic aperture (e_h) could be obtained by back calculation based on the cubic law, which can be defined as follows (Snow, 1969):

$$e_h = \sqrt[1/3]{\left(\frac{12\mu Q}{w\,\nabla P}\right)}, \quad (1)$$

where μ is the viscosity of water, w is the fracture width and and ∇P is the pressure gradient. The cubic law is valid for laminar flow through parallel wall fractures with fairly smooth surfaces. When assessing the flow characteristics of a rock fracture, the Reynolds number (Re), which is defined as the ratio of inertial forces to viscous forces, is typically used to quantify the onset of nonlinear flow, where ρ is the fluid density (Schlichting, 1968):

$$Re = \frac{\rho Q}{\mu w} \quad (2)$$

3 Result and Discussion

The point clouds which were made by photogrammetry methods are shown in Fig. 7. According to Fig. 2, the profiles are shown with the red lines for the bottom and top pairs of the sample. Profilometer and photogrammetry were used to assess the roughness of fracture surfaces. The subjectively assessed scale corrected JRC values for top and both ranged from 6-10 JRC and showed no significant anisotropy (Fig. 8 on left). The digital photogrammetry profiles (Fig. 8 on right) are visibly more accurate than the profiles obtained manually using a profilometer.

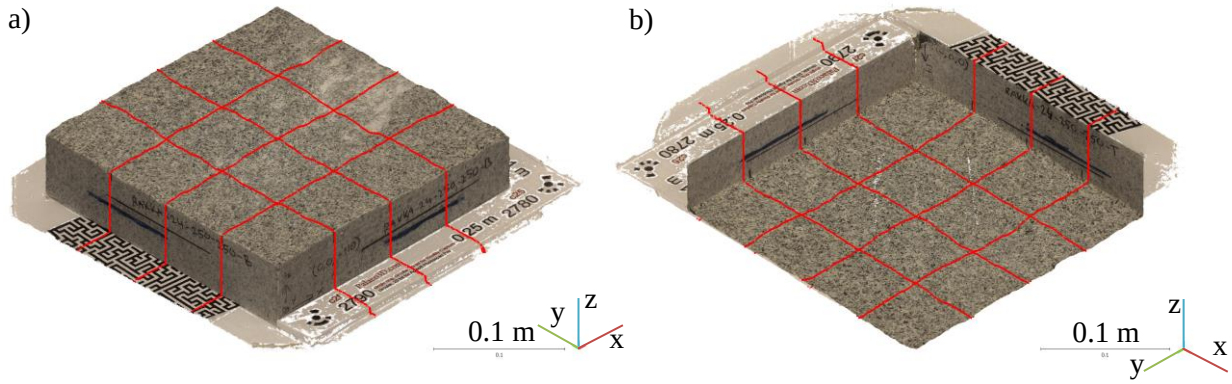

Fig. 7. The red lines show where the cross-sectional profiles were extracted for sample RAKKA-24 bottom (a) and top (b).

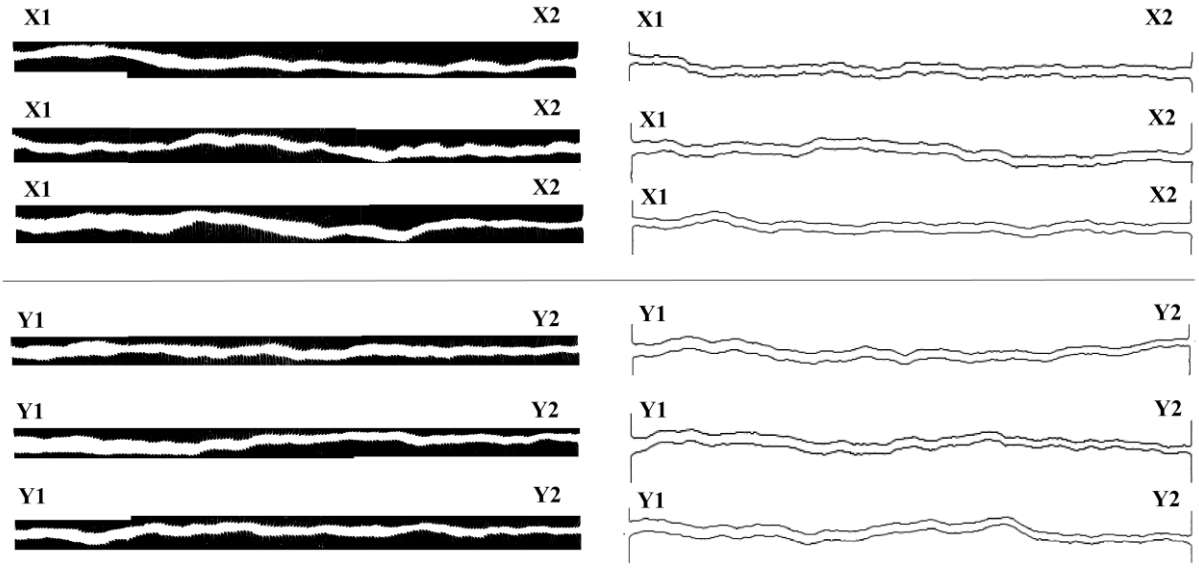

Fig. 8. Extracted 250 mm long profiles using profilometer (on left) and photogrammetry (on right).

In order to distinguish the distribution of flow in the fracture plane, the average flow rate volume per minute between two directions X and Y at inlet and outlet boundaries with same situations before and after loading normal stress were illustrated in Fig. 9. Although there are some fluctuations for the former data, the flow rates were constant among the latter. In all situations, the amounts of water flow in the direction Y were more than in the direction X. This indicates anisotropic behaviour of the hydraulic flow.

All water pressure gradient can be considered as laminar follow regimes because the calculated Reynolds numbers are less than 2300 and using cubic law is acceptable (Table 1). Hydraulic apertures in the directions X and Y before and after applying external normal stress are tabulated in Table 1.

Table 1. Reynolds numbers and hydraulic apertures in directions X and Y

Water pressure gradient (bar)	Before applying external normal stress				After applying normal stress (0.2 MPa)			
	Direction X		Direction Y		Direction X		Direction Y	
	e_h (mm)	Re	e_h (mm)	Re	e_h (mm)	Re	e_h (mm)	Re
1	0.0168	50.19	0.0169	50.94	0.0162	44.94	0.0165	47.27
3	0.0213	101.87	0.0216	105.62	0.0212	100.37	0.0213	101.12
5	0.0236	137.83	0.0237	139.33	0.0235	136.33	0.0236	138.58

There are no prominent differences between directions X and Y. However, the amount of water that passes through direction X is greater than direction Y. To recognize flow paths when water moves through a joint the three-way frame was used. Water with different pressures was injected into the sample from direction X or Y and the water coming out from three sides was measured (Figs. 5 and 6). Corresponding water volumes per minute are shown in Figs. 10 and 11. The minimum amounts were related to the straight direction since water should pass a long way to reach the other side. Figure 10 shows the proportion of outflows was Y1 > Y2 > X2 before loading normal stress. However, after loading normal stress, these amounts changed to Y2 > Y1 > X2. It might be related to joint asperity distribution (Fig. 8). Before loading normal stress, this allows a high amount of water to go through the inside of the Y2 rather than Y1. After loading test, the asperity distribution in the side of Y2 was well-matched while the side of Y1 asperities could not match together perfectly. Owing to this reason, the collected water from the side Y1 increased. Based on unmatched asperity, the amounts of collected water from both sides of X increased after loading normal stress. Because the first part of the joint was related to Y1 and it was not well-matched, but the other side (Y2) matched. The direction Y shows a similar tendency where the majority of the flow goes to the side drains X2 and X1 (Figure 11).

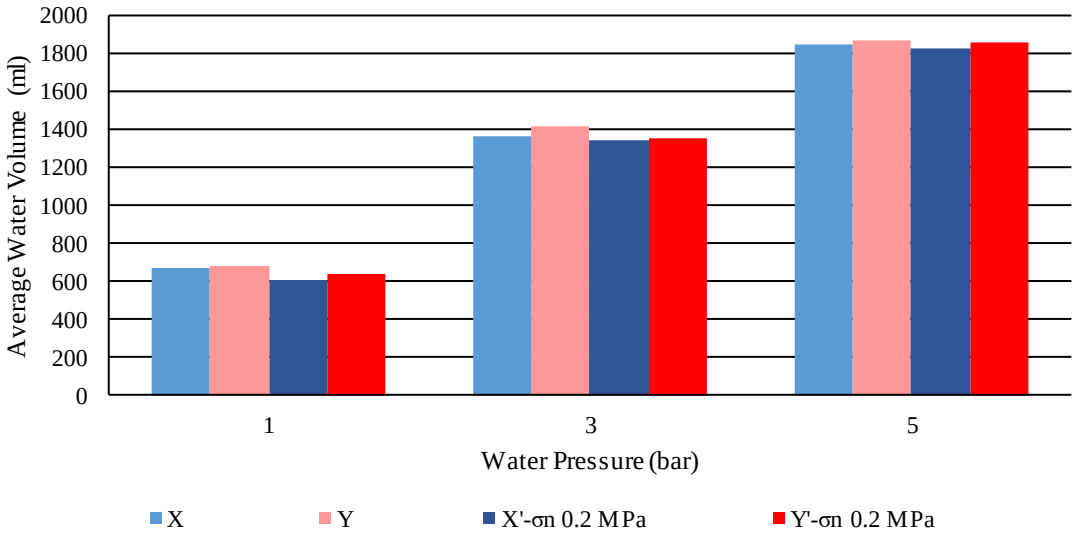

Fig. 9. Comparison of flow rate in different directions before and after loading normal pressure.

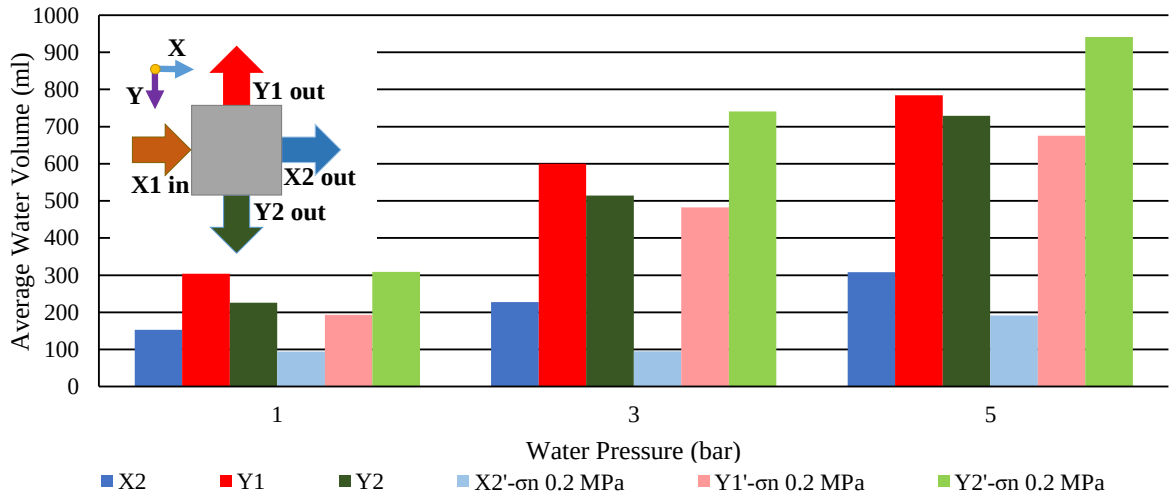

Fig. 10. Comparison of flow rate before and after loading normal pressure direction X.

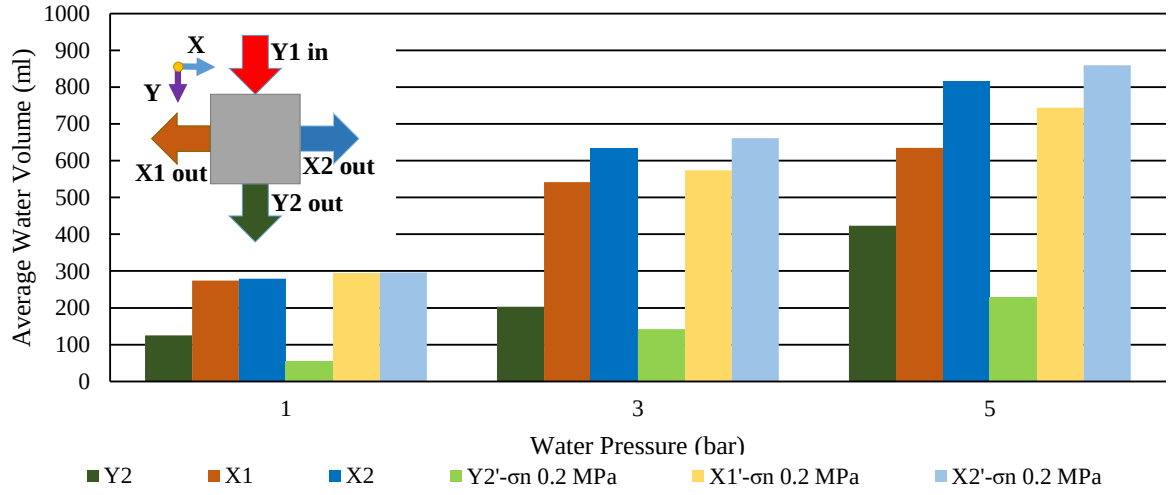

Fig. 11. Comparison of flow rate before and after loading normal pressure direction Y.

4 Conclusion

Structure-from-Motion photogrammetry was used to measure the surface roughness of Kuru gray granite slabs pair with a mechanically induced tensile fracture between the slabs. The photogrammetric method as described in this paper can be utilized to digitize the rock fracture geometry at submillimeter resolution. Cross-sections extracted from the digitized fracture surface are more precise than the manually obtained measurements using a profilometer. The digital fracture profiles can be used as initial geometry for predictive numerical modelling.

The presented new experimental three-way fluid flow cell has successfully been used to characterize the fluid flow of a 250 mm x 250 mm fracture surface. Based on the preliminary results without external normal stress, the fluid flow in all three directions is proportional to the fluid pressure. With the introduction of a 0.2 MPa normal stress, the fluid flow tends to exit at the sides of the sample and the linear flow through the sample is reduced. This means that diagonal components of permeability are significantly stress-dependent compared to the off-diagonal terms for this sample size.

Together the new digitization method and the new experimental setup allow the contactless characterization of hydro-mechanical properties of rock fractures and the experimental validation of the results using the three-way fluid flow tests. The presented results are the initial set of experimental hydromechanical test results for 250 mm x 250 mm scale and continuation of tests in 500 mm x 500 mm and 1000 mm x 1000 mm sample sizes with normal stress are the next steps during 2019-2022.

References

Bandis, S., Lumsden, A. C. & Barton, N. R. 1981. Experimental studies of scale effects on the shear behaviour of rock joints. In International journal of rock mechanics and mining sciences & geomechanics abstracts (Vol. 18, No. 1, pp. 1-21). Pergamon.

Barton, N.R. & Choubey, V. 1977. The shear strength of rock joints in theory and practice. Rock Mechanics. Vol. 10:1-2. S. 1-54.

Brown, S., Caprihan, A. & Hardy, R. 1998. Experimental observation of fluid flow channels in a single fracture. Journal of Geophysical Research: Solid Earth, 103(B3), 5125-5132.

Ferer, M., Crandall, D., Ahmadi, G. & Smith, D. H. 2011. Two-phase flow in a rough fracture: Experiment and modeling. Physical Review E, 84(1), 016316.

International Society for Rock Mechanics Commission on Standardisation of Laboratory and Field Tests. 1978. Suggested methods for the quantitative description of discontinuities in rock masses. Int. J. Rock Mech. Min. Sci. & Geomech. Abstr. Vol. 15. S. 319-368.

Isakov, E., Ogilvie, S. R., Taylor, C. W. & Glover, P. W. 2001. Fluid flow through rough fractures in rocks I: high resolution aperture determinations. Earth and Planetary Science Letters, 191(3-4), 267-282.

Jaeger, J. C., Cook, N. G. & Zimmerman, R. 2007. Fundamentals of rock mechanics. 4th ed. John Wiley & Sons.

Jiang, Y., Li, B. & Tanabashi, Y. 2006. Estimating the relation between surface roughness and mechanical properties of rock joints. International Journal of Rock Mechanics and Mining Sciences, 43(6), 837-846.

Jiang, Y., Xiao, J., Tanabashi, Y. & Mizokami, T. 2004. Development of an automated servo-controlled direct shear apparatus applying a constant normal stiffness condition. Int. J. Rock Mech. Min. Sci., 41(2), 275-286.

Lee, H. S. & Cho, T. F. 2002. Hydraulic characteristics of rough fractures in linear flow under normal and shear load. Rock Mechanics and Rock Engineering, 35(4), 299-318.

Li, B., Jiang, Y., Koyama, T., Jing, L. & Tanabashi, Y. 2008. Experimental study of the hydro-mechanical behavior of rock joints using a parallel-plate model containing contact areas and artificial fractures. International Journal of Rock Mechanics and Mining Sciences, 45(3), 362-375.

Min, K. B., Rutqvist, J., Tsang, C. F. & Jing, L. 2004. Stress-dependent permeability of fractured rock masses: a numerical study. International Journal of Rock Mechanics and Mining Sciences, 41(7), 1191-1210.

Nemoto, K., Watanabe, N., Hirano, N. & Tsuchiya, N. 2009. Direct measurement of contact area and stress dependence of anisotropic flow through rock fracture with heterogeneous aperture distribution. Earth and Planetary Science Letters, 281(1-2), 81-87.

Noorishad, J. & Tsang, C. F. 1996. Coupled thermohydroelasticity phenomena in variably saturated fractured porous rocks--formulation and numerical solution. In Developments in geotechnical engineering (Vol. 79, pp. 93-134). Elsevier.

Ogilvie, S. R., Isakov, E. & Glover, P. W. 2006. Fluid flow through rough fractures in rocks. II: A new matching model for rough rock fractures. Earth and Planetary Science Letters, 241(3-4), 454-465.

Rong, G., Yang, J., Cheng, L. & Zhou, C. 2016. Laboratory investigation of nonlinear flow characteristics in rough fractures during shear process. Journal of hydrology, 541, 1385-1394.

Rutqvist, J. & Stephansson, O. 2003. The role of hydromechanical coupling in fractured rock engineering. Hydrogeology Journal, 11(1), 7-40.

Saito, R., Ohnishi, Y., Nishiyama, S., Yano, T. & Uehara, S. 2005. Hydraulic characteristics of single rough fracture under shear deformation. In ISRM International Symposium-EUROCK 2005. ISRM.

Şen, Z. & Sadagah, B. H. 2002. Probabilistic horizontal stress ratios in rock. Mathematical geology, 34(7), 845-855.

Wang, C., Jiang, Y., Luan, H., Liu, J. & Sugimoto, S. 2019. Experimental Study on the Shear-Flow Coupled Behavior of Tension Fractures Under Constant Normal Stiffness Boundary Conditions. Processes, 7(2), 57.

Yasuhara, H., Polak, A., Mitani, Y., Grader, A. S., Halleck, P. M. & Elsworth, D. 2006. Evolution of fracture permeability through fluid–rock reaction under hydrothermal conditions. Earth and Planetary Science Letters, 244(1-2), 186-200.

Yeo, I. W., De Freitas, M. H. & Zimmerman, R. W. 1998. Effect of shear displacement on the aperture and permeability of a rock fracture. Int. J. Rock Mech. Min. Sci., 35(8), 1051-1070.

Zimmerman, R. & Main, I. 2004. Hydromechanical behaviour of fractured rocks. International Geophysics Series, 89, pp. 363-422.